



King's Research Portal

DOI:

[10.1021/acs.jpcllett.8b01494](https://doi.org/10.1021/acs.jpcllett.8b01494)

Document Version

Peer reviewed version

[Link to publication record in King's Research Portal](#)

Citation for published version (APA):

Wang, Y. J., Rico-Lastres, P., Lezamiz, A., Mora, M., Solsona, C., Stirnemann, G., & Garcia-Manyes, S. (2018). DNA Binding Induces a Nanomechanical Switch in the RRM1 Domain of TDP-43. *Journal of physical chemistry letters*, 9(14), 3800-3807. <https://doi.org/10.1021/acs.jpcllett.8b01494>

Citing this paper

Please note that where the full-text provided on King's Research Portal is the Author Accepted Manuscript or Post-Print version this may differ from the final Published version. If citing, it is advised that you check and use the publisher's definitive version for pagination, volume/issue, and date of publication details. And where the final published version is provided on the Research Portal, if citing you are again advised to check the publisher's website for any subsequent corrections.

General rights

Copyright and moral rights for the publications made accessible in the Research Portal are retained by the authors and/or other copyright owners and it is a condition of accessing publications that users recognize and abide by the legal requirements associated with these rights.

- Users may download and print one copy of any publication from the Research Portal for the purpose of private study or research.
- You may not further distribute the material or use it for any profit-making activity or commercial gain
- You may freely distribute the URL identifying the publication in the Research Portal

Take down policy

If you believe that this document breaches copyright please contact librarypure@kcl.ac.uk providing details, and we will remove access to the work immediately and investigate your claim.

DNA Binding Induces a Nanomechanical Switch in the RRM1 Domain of TDP-43

Yongjian Wang, Palma Rico-Lastres, Ainhoa Lezamiz, Marc Mora, Carles Solsona, Guillaume Stirnemann, and Sergi Garcia-Manyes

J. Phys. Chem. Lett., **Just Accepted Manuscript** • DOI: 10.1021/acs.jpcllett.8b01494 • Publication Date (Web): 20 Jun 2018

Downloaded from <http://pubs.acs.org> on June 21, 2018

Just Accepted

“Just Accepted” manuscripts have been peer-reviewed and accepted for publication. They are posted online prior to technical editing, formatting for publication and author proofing. The American Chemical Society provides “Just Accepted” as a service to the research community to expedite the dissemination of scientific material as soon as possible after acceptance. “Just Accepted” manuscripts appear in full in PDF format accompanied by an HTML abstract. “Just Accepted” manuscripts have been fully peer reviewed, but should not be considered the official version of record. They are citable by the Digital Object Identifier (DOI®). “Just Accepted” is an optional service offered to authors. Therefore, the “Just Accepted” Web site may not include all articles that will be published in the journal. After a manuscript is technically edited and formatted, it will be removed from the “Just Accepted” Web site and published as an ASAP article. Note that technical editing may introduce minor changes to the manuscript text and/or graphics which could affect content, and all legal disclaimers and ethical guidelines that apply to the journal pertain. ACS cannot be held responsible for errors or consequences arising from the use of information contained in these “Just Accepted” manuscripts.



DNA Binding Induces a Nanomechanical Switch in the RRM1 Domain of TDP-43

*Yong Jian Wang^{†,#}, Palma Rico-Lastres^{†,#}, Ainhoa Lezamiz^{†,#}, Marc Mora[†], Carles Solsona[‡],
Guillaume Stirnemann[&] and Sergi Garcia-Manyes^{†,*}*

[†] Department of Physics and Randall Centre for Cell and Molecular Biophysics, King's College
London, WC2R 2LS, London, UK.

[‡] Department of Pathology and Experimental Therapeutics, Faculty of Medicine and Health
Sciences, University of Barcelona and Bellvitge Biomedical Research Institute (IDIBELL)
L'Hospitalet de Llobregat, Barcelona 08907, Spain

[&] CNRS Laboratoire de Biochimie Théorique, Institut de Biologie Physico-Chimique, Univ.
Paris Denis Diderot, Sorbonne Paris Cité, PSL Research University, 75005 Paris, France

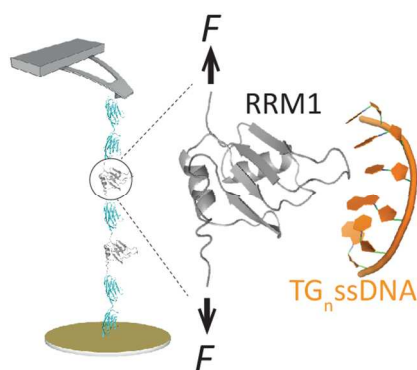
These authors contributed equally to the work

Corresponding Author

* sergi.garcia-manyes@kcl.ac.uk.

1
2
3 ABSTRACT. Understanding the molecular mechanisms governing protein-nucleic acid
4 interactions is fundamental to many nuclear processes. However, how nucleic acid binding
5 affects the conformation and dynamics of the substrate protein remains poorly understood. Here
6 we use a combination of single molecule force spectroscopy AFM and biochemical assays to
7 show that the binding of TG-rich ssDNA triggers a mechanical switch in the RRM1 domain of
8 TDP-43, toggling between an entropic spring devoid of mechanical stability and a shock
9 absorber bound-form that resists unfolding forces of ~ 40 pN. The fraction of mechanically
10 resistant proteins correlates with an increasing length of the TG_n oligonucleotide, demonstrating
11 that protein mechanical stability is a direct reporter of nucleic acid binding. Steered Molecular
12 Dynamics simulations on related RNA oligonucleotides reveal that the increased mechanical
13 stability fingerprinting the holo-form is likely to stem from a unique scenario whereby the
14 nucleic acid acts as a “mechanical staple” that protects RRM1 from mechanical unfolding. Our
15 approach highlights nucleic acid binding as an effective strategy to control protein
16 nanomechanics.

39 TOC GRAPHICS



1
2
3 **KEYWORDS.** Single-molecule studies, RRM1 domain, Nucleotides, Mechanical properties,
4
5 Nucleic acid binding.
6
7
8
9

10 The nanomechanical properties of individual proteins regulate a number of major
11 biological processes, including the deformability of the extracellular matrix¹, mechanotrans
12 duction in focal adhesion adaptors², the elasticity of cardiac titin³ or the degradation of proteins
13 in the proteasome⁴⁻⁵. Several molecular tactics have been convincingly used to modify the
14 mechanical stability of proteins; beyond simple protein unfolding —which converts the
15 mechanically resistant native state into a compliant and extended protein conformation⁶—, the
16 introduction of key point mutations in the so-called “mechanical clamp”⁷ and the presence of
17 stiff disulfide bonds⁸⁻⁹ or covalent organometallic bonds¹⁰⁻¹¹ have all been shown to have a
18 direct effect on the mechanical stability of the natively folded conformation.
19
20
21
22
23
24
25
26
27
28
29
30

31
32
33 In addition to these more common strategies, ligand binding¹² has recently emerged as an
34 effective orthogonal modulator of protein nanomechanics. For example, DHFR was shown to
35 increase its mechanical stability upon binding nicotinamide adenine dihydrogen phosphate
36 (NADPH), 7,8-dihydrofolate (DHF) or inhibitor methotrexate (MTX), converting a purely elastic
37 protein devoid of mechanical stability into an efficient shock absorber able to withstand
38 stretching forces¹³. Likewise, the enzyme staphylococcal nuclease increases its mechanical
39 resistance upon binding its inhibitor deoxythymidine 3',5'- bisphosphate¹⁴. Similarly, binding of
40 small sugars (in the case of maltose binding protein¹⁵⁻¹⁶, the hyperthermophilic adenine
41 diphosphate (ADP)-dependent glucokinase¹⁷ and membrane transporters¹⁸) or single amino acids
42 (such as leucine¹⁹) can change both the height of the energy barriers and the distribution of
43
44
45
46
47
48
49
50
51
52
53
54
55
56
57
58
59
60

1
2
3 unfolding pathways. In addition, metal binding has also revealed as a successful strategy to
4 regulate protein stiffness through calcium²⁰⁻²³ or nickel²⁴⁻²⁵ binding. Perhaps even more
5 conspicuous are the mechanical consequences of small peptide —or full protein— binding. In
6 this vein, the mechanical properties of protein G are substantially increased upon binding the IgG
7 antibody²⁶. Furthermore, SUMO1 increases its mechanical stability upon binding small
8 peptides²⁷. Similarly, the attachment of the short hydrophobic APPY polypeptide induces
9 selective increase of the mechanical properties of the domain I of the multidomain DnaJ
10 chaperone²⁸. Other recent examples epitomise the importance of mechanically revealing key
11 binding pockets that are otherwise hidden in the folded conformation^{29 30-32}.

22
23
24
25
26 Collectively, these experiments revealed the large knock-on effects that protein-protein
27 interactions have on protein nanomechanics. This growing experimental evidence makes it
28 tempting to speculate that, given the increasingly large number of identified DNA- and RNA-
29 binding proteins (DRBPs)³³, nucleic acid binding, further to modifying unfolding pathways³⁴,
30 might play an analogous role in regulating the mechanical stability of proteins. Direct testing of
31 this hypothesis has remained elusive, mostly due to the lack of an extensive pool of DNA-
32 binding proteins for which the crystal structure in the apo- and holo- forms has been solved, and
33 especially given the difficulty to obtain these proteins biochemically free of the nucleic acid
34 partner. Here, we investigated how nucleic acids of well-defined sequences regulate the
35 nanomechanical properties of the RRM1 domain of the 43 kDa TAR DNA-binding protein
36 (TDP-43). TDP-43 plays important roles in many essential cellular functions involved in DNA
37 transcription and RNA translation³⁵, and it is hence capable of binding both RNA and DNA.
38 Furthermore, TDP-43 has been associated to several important neurodegenerative disorders,
39
40
41
42
43
44
45
46
47
48
49
50
51
52
53
54
55
56
57
58
59
60

1
2
3 including amyotrophic lateral sclerosis (ALS) and frontotemporal lobar degeneration (FTLD)³⁶⁻
4
5 ³⁸. Under physiological conditions, TDP-43 is predominantly localised in the nucleus with low
6
7 levels in the cytoplasm³⁹⁻⁴⁰ and conducts a multiplex of functionalities, being involved in
8
9 different steps of RNA processing including transcription, mRNA splicing, transport and
10
11 translation, and works as a transcription factor as well⁴¹. Given its multifunctional role, accessing
12
13 the microscopic insights underpinning the protein-nucleic acid interaction is of capital
14
15 importance towards establishing a link between function and protein conformation. From the
16
17 topological perspective, TDP-43 is composed of two tandem RNA recognition motifs (RRM1
18
19 and RRM2) flanked between an N-terminal domain (NTD), an NLC segment that has been
20
21 reported to bind RNA⁴², and the C-terminal glycine-rich domain (GRD, Figure 1a)⁴³. The crystal
22
23 structure of both RRM domains has been solved in complex to different UG- and TG- rich
24
25 single-stranded RNA and DNA sequences⁴⁴, concluding that RRM1 plays a dominant role in
26
27 nucleic acid binding whereas RRM2 holds a supporting function⁴⁵. Given its ability to effectively
28
29 bind DNA and RNA, and thanks to the fact that its binding properties have been characterised
30
31 both structurally and biochemically, RRM1 emerges as an excellent case study to elucidate how
32
33 nucleic acid binding has direct effects on protein conformation.
34
35
36
37
38
39
40
41

42 Using single molecule force spectroscopy in combination with biochemistry assays, here
43
44 we demonstrate that DNA binding has a major effect on the mechanical properties of the RRM1
45
46 domain of TDP-43, triggering its transition from a compliant, entropic spring into a mechanically
47
48 resistant shock absorber. Supporting Molecular Dynamics simulations reveal that such a
49
50 mechanical switch results from a unique molecular strategy whereby the nucleic acid functions
51
52 as a ‘molecular lid’ that protects the RRM1 domain from mechanical unfolding.
53
54
55
56
57
58
59
60

1
2
3 To investigate the mechanical properties of the apo-RRM1 domain, we constructed a
4 polyprotein containing two RRM1 monomers, each one flanked by three titin I27th Ig domains
5 that serve as standard molecular fingerprints, resulting in the [I27₂-RRM1-I27-RRM1-I27₂]
6 polyprotein (Figure 1a). A multistep elution protocol ensured quantitative removal of DNA⁴⁶,
7 confirmed by the low (~0.6) ratio of absorbance measured at 260/280 nm, a generally accepted
8 signature of quantitative removal of DNA⁴⁶. Individual polyproteins were stretched under a
9 constant velocity of 400 nm s⁻¹ using an atomic force spectrometer (AFM). The resulting force-
10 extension trajectories exhibited a first feature-less protein extension (associated to a total contour
11 length, $L_T = 81$ nm) followed by the well-characterised unfolding of the I27 protein, occurring at
12 forces ~200 pN and hallmarked by $\Delta L_{I27} = 28$ nm⁴⁷ (Figure 1c). Having learnt that apo-RRM1 is
13 void of mechanical stability, we sought to examine whether the addition of TG₁₅, which
14 effectively binds RRM1 as revealed by electrophoretic mobility shift assays (EMSA, Figure 1b),
15 has an effect on the nanomechanical properties of RRM1. The individual unfolding trajectories
16 (Figure 1d) show that, in sharp contrast to the apo-form, mechanical unfolding of the holo-
17 RRM1 results in a well-defined force peak occurring at forces $F = 39 \pm 11$ pN that occurs
18 concomitant with an increment in contour length of $\Delta L = 28 \pm 1$ nm (Figure S1), which is
19 consistent with the complete extension of the RRM1 domain ($77\text{aa} \times 0.38^6$ nm/aa – folded
20 length(1.3nm) =27.96 nm) after mechanical unfolding. A gallery of individual unfolding
21 trajectories for both the apo- and holo- proteins forms is shown in the Figure S2. To further
22 confirm that the unfolding events observed in Figure 1d corresponds to the DNA-mediated
23 mechanical stabilisation of RRM1, we repeated the same experiments in the presence of CA₁₅,
24 which does not quantitatively bind RRM1 (Figure 1b)⁴⁸⁻⁴⁹. Under these control conditions, the
25
26
27
28
29
30
31
32
33
34
35
36
37
38
39
40
41
42
43
44
45
46
47
48
49
50
51
52
53
54
55
56
57
58
59
60

individual unfolding trajectories lacked the well-defined force peak (Figure 1e), hence mostly recapitulating the behaviour of apo-RRM1.

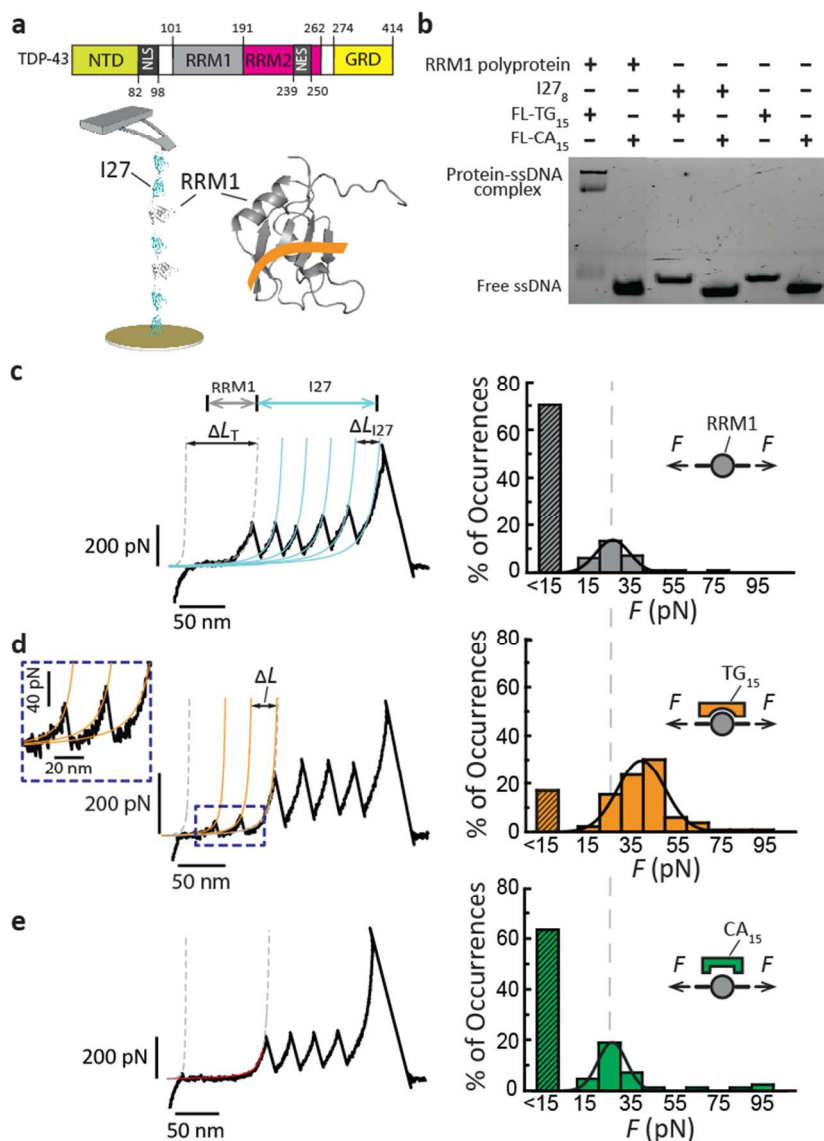
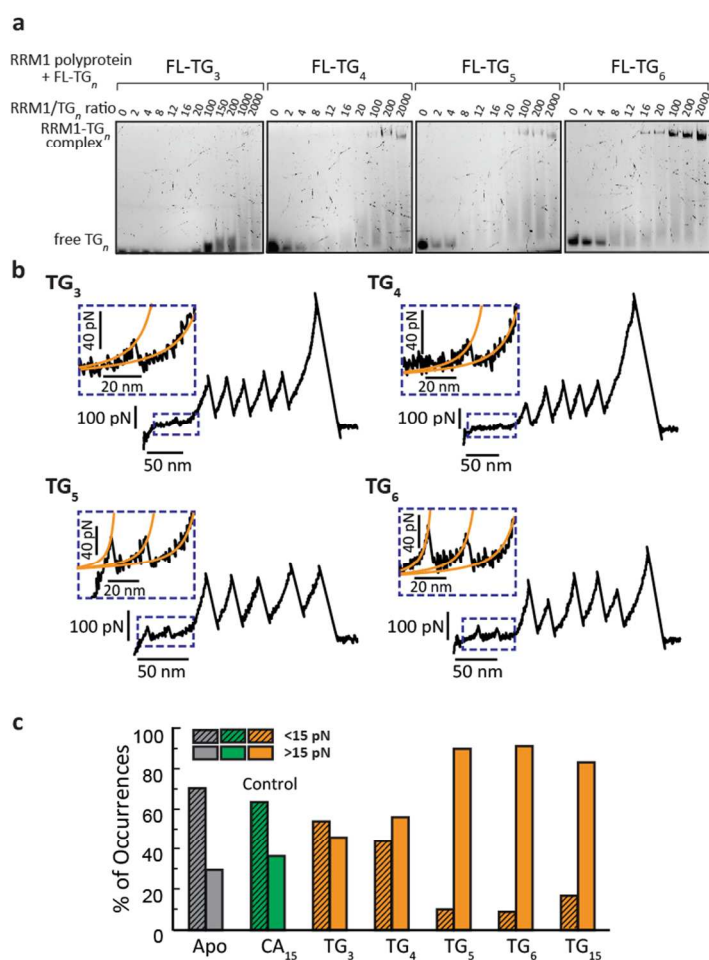


Figure 1. (a) Schematic representation of the TDP-43 protein, composed of two non-equivalent RRM domains. A polyprotein containing two RRM1 (grey) domains, [I27₂-RRM1-I27-RRM1-I27₂], is stretched between a gold surface and an AFM cantilever tip, and its nanomechanical

1
2
3 properties were tested upon oligonucleotide binding (orange, PDB: 4BS2). (b) DNA specificity
4 assay monitored by EMSA performed on RRM1 and I27₈ polyprotein constructs upon addition
5 of different FL ssDNA oligonucleotides. The amount of DNA and protein was maintained fixed
6 (10 nM and 80 nM, respectively, in a 14 μ l load). The binding assay was performed in a 25 mM
7 HEPES pH 7.4 buffer solution. (c) *Left*: Individual unfolding trajectory of the [I27₂-RRM1-I27-
8 RRM1-I27₂] polyprotein, exhibiting a first feature-less extension corresponding to the unfolding
9 of the RRM1 domains followed by the unfolding of the I27 markers, occurring at forces \sim 200
10 pN. *Right*: Histogram of the forces required to unfold the apo-RRM1 domain, demonstrating that
11 in \sim 70% of the unfolding events ($n = 69$) the apo-RRM1 form unfolds in the absence of
12 mechanical stability. (d) Upon addition of \sim 1.5 μ M of ssTG₁₅ oligonucleotide, the mechanical
13 unfolding of the holo-RRM1 domain can be fingerprinted by a saw-tooth pattern, with the
14 unfolding peaks occurring at forces \sim 39 pN and concomitant to an increment in contour length of
15 $\Delta L \sim$ 28 nm, $n = 113$. (e) Analogous control experiments using a CA₁₅ oligonucleotide ($n = 54$),
16 which do not quantitatively bind RRM1, exhibit unfolding trajectories devoid of mechanical
17 stability that recapitulate the apo-form.
18
19
20
21
22
23
24
25
26
27
28
29
30
31
32
33
34
35
36
37
38
39
40

41 Inspired by recent biochemistry findings⁴⁹⁻⁵⁰, we then asked whether the length of (TG)-
42 containing ssDNA oligonucleotides has an effect on RRM1 binding in our experimental
43 conditions. To address this question, electrophoretic mobility shift assays were used to
44 characterise the binding of fluorescently-labelled (henceforth, FL) TG₃, TG₄, TG₅, TG₆,
45 TG₁₅ oligonucleotides (10 nM) with increasing stoichiometric ratios of the [I27₂-RRM1-I27-
46 RRM1-I27₂] polyprotein (Figure 2a). These experiments demonstrated that longer TG
47 oligonucleotides require a lower protein:DNA ratio to induce quantitative binding (Figure 2a and
48
49
50
51
52
53
54
55
56
57
58
59
60

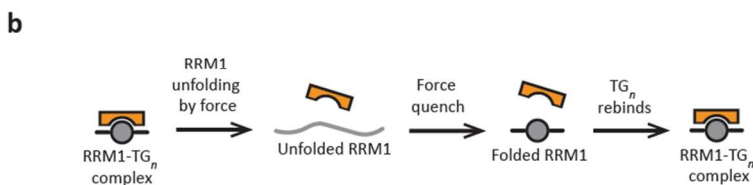
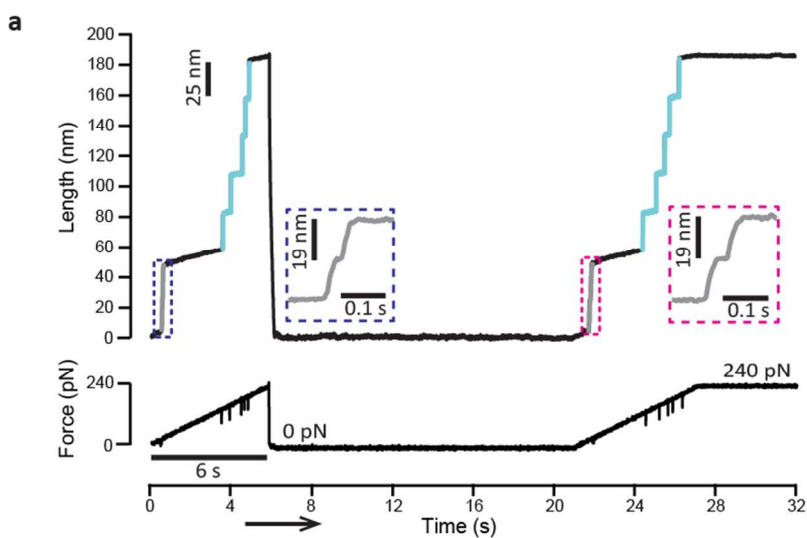
Figure S3). To test whether the measured binding efficiency directly correlates with the DNA-induced mechanical stabilization of RRM1, we examined the mechanical behaviour of RRM1 when exposed to different TG-containing ssDNA oligomers of varying lengths. Crucially, in all cases we observed signatures of mechanical stabilization of RRM1 (Figure 2b, Figure S4). Remarkably, the fraction of trajectories displaying a mechanical peak increased with the number of TG repetitions, with a significant transition towards the bound fraction for $TG_n > 5$ (Figure 2c), thus recapitulating the binding titration measured in Figure 2a. Altogether, these experiments suggest that the change in mechanical stability of RRM1 is a direct read-out of DNA binding.



1
2
3 **Figure 2.** (a) Protein:DNA titrations monitored by EMSA. FL TG₃, TG₄, TG₅ and TG₆ ssDNA
4 oligonucleotides (10 nM) titrated with increasing amounts of the RRM1 polyprotein construct in
5 25 mM HEPES pH 7.4 buffer. Values on the top of the gel indicate the RRM1:DNA ratio. (b)
6 Individual unfolding trajectories corresponding to the unfolding of RRM1 domains in the
7 presence of TG₃, TG₄, TG₅, and TG₆ single stranded oligonucleotides, exhibiting force peaks
8 corresponding to the forced unfolding. (c) Histogram corresponding to the % of individual
9 unfolding events ($n = 40-140$) featuring mechanical stability under all tested conditions, with the
10 % increasing with the length of the TG_{*n*} oligonucleotide.
11
12
13
14
15
16
17
18
19
20
21
22
23
24
25

26 We next set out to probe whether the recovery of mechanical stability through DNA
27 binding is a reversible process intricately linked to mechanical refolding. To this purpose, we
28 conducted force-quench experiments (which afford superior control of the folding dynamics)⁵¹ in
29 the presence of TG₁₅, whereby the force was first ramped up to 240 pN at a constant rate of 40 pN
30 s⁻¹ to trigger the unfolding of holo-RRM1 (fingerprinted by a step-wise increase of protein length
31 of 19 ± 1 nm, occurring at $F = 30 \pm 8$ pN, Figure S5), followed by the unfolding of the I27
32 domains, marked by the increase of the protein's contour length in ~ 25 nm steps (Figure 3a). The
33 force was subsequently withdrawn for $t_q = 15$ s to trigger protein refolding before the force was
34 ramped up again to test the folding status of the protein. Remarkably, in ~ 46 % of the trajectories
35 ($n = 13$), mechanically re-stretching of the protein mirrored the initial unfolding sequence
36 whereby the mechanically resistant RRM1 was first unfolded, prior to the unfolding of the I27
37 domains occurring at higher forces. The recovery of mechanical stability for RRM1 suggests
38 that, upon refolding, RRM1 is able to effectively re-bind TG₁₅. Similar conclusions were
39
40
41
42
43
44
45
46
47
48
49
50
51
52
53
54
55
56
57
58
59
60

1
 2
 3 qualitatively reached in the case of TG₆ binding (Figure S6). Two distinct scenarios could
 4 mechanistically explain the rebinding process; either DNA was not removed from the protein
 5 and kept bound after unfolding, or alternatively DNA was able to re-bind from the solution
 6 and kept bound after unfolding, or alternatively DNA was able to re-bind from the solution
 7 within the experimental quench time (Figure 3b). Discriminating between both possibilities
 8 would eventually require an extensive set of experiments where both the quench time and also
 9 the time the mechanically unfolded protein is exposed to the solvent environment are
 10 independently varied. Repeating the experiments over a range of protein concentrations could
 11 also help elucidate whether or not nucleic acids remain bound after RRM1 mechanical unfolding.
 12 While these experiments are beyond the scope of the present work, our results highlight the
 13 reversibility of the binding process on experimental timescales, fingerprinted by the recovery of
 14 the RRM1 mechanical stability.
 15
 16
 17
 18
 19
 20
 21
 22
 23
 24
 25
 26
 27
 28
 29
 30
 31
 32
 33
 34
 35
 36
 37
 38
 39
 40
 41
 42
 43
 44
 45
 46
 47
 48
 49
 50
 51
 52
 53
 54
 55
 56
 57
 58
 59
 60

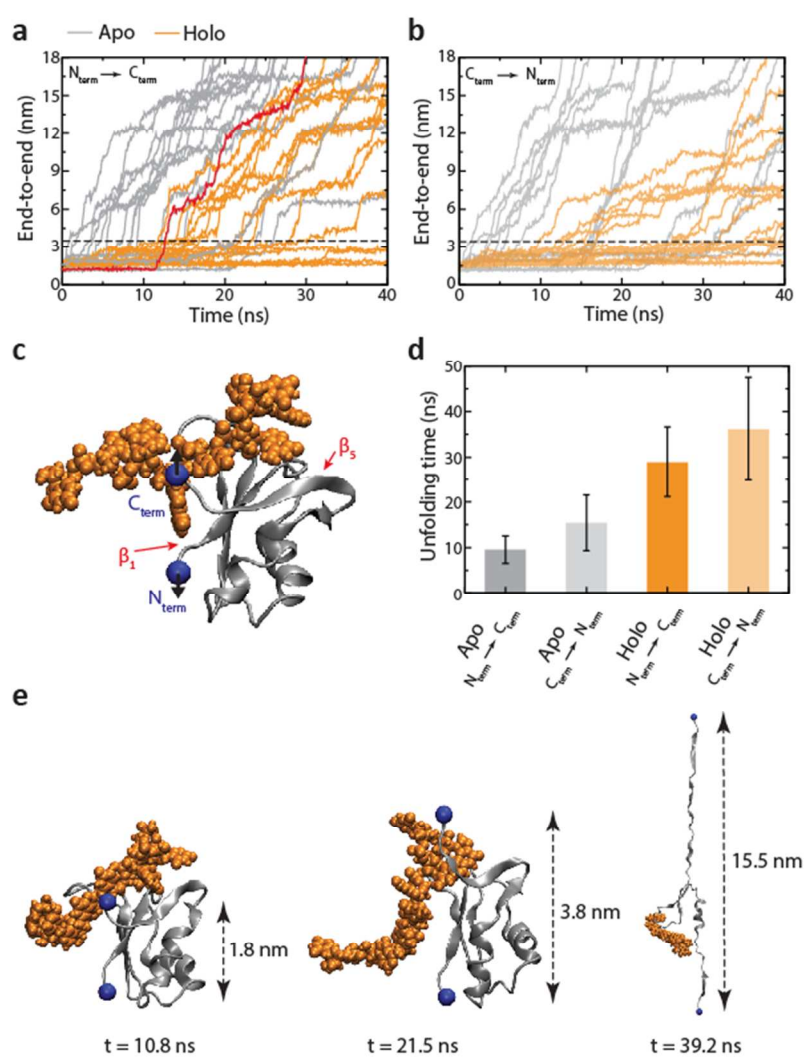


1
2
3 **Figure 3.** (a) Individual refolding trajectory ($n = 13$) of a single [I27₂-RRM1-I27-RRM1-I27₂]
4 polyprotein in the presence of TG₁₅ following a force-quench protocol. During the first 6
5 seconds, the protein was stretched at a constant loading rate of 40 pN s⁻¹. This first force-ramp
6 pulse elicited the initial unfolding of the RRM1 domain, fingerprinted by the presence of steps of
7 19 ± 1 nm (grey) and occurring at forces 30 ± 8 pN. The mechanical unfolding of the I27 marker
8 occurred at higher forces ~150-210 pN concomitant to a protein 25 nm-stepwise length increase
9 (blue). Once the protein reached a stretching force of 240 pN, the force was completely removed
10 for $t_q = 15$ s to trigger protein refolding. The *test* pulse, mirroring the first force-ramp protocol,
11 probes the folding status of the protein. Upon re-stretching the protein at a constant rate of 40 pN
12 s⁻¹, RRM1 re-unfolded as hallmarked by the presence of 19 nm steps, followed by the re-
13 unfolding of the I27 domains. The complete recovery of mechanical stability of the RRM1
14 domain is an unambiguous proxy for the successful (i) refolding of the protein and the
15 subsequent rebinding of the TG₁₅ ssDNA oligonucleotide. (b) Two possible scenarios could
16 account for the unbinding and rebinding of TG₁₅ under force. In the first scenario, upon protein
17 unfolding, the ssDNA would be completely removed. In this case, rebinding a ssDNA molecule
18 from solution would occur during the quench time. Alternatively, after mechanical unfolding the
19 TG₁₅ oligonucleotide might remain attached to RRM1, facilitating the conformational search for
20 re-binding upon removal of the pulling force.
21
22
23
24
25
26
27
28
29
30
31
32
33
34
35
36
37
38
39
40
41
42
43
44
45
46
47
48
49
50
51
52
53
54
55
56
57
58
59
60

To obtain an atomistic picture of the mechanism by which DNA enhances the mechanical unfolding of RRM1, we conducted Steered Molecular Dynamics (SMD) simulations under constant force conditions (Figure 4). Lacking the structure of the RRM1 bound to the DNA TG sequence, we used instead as a proxy the RRM1 structure bound to the RNA sequence

1
2
3 (5'-GUGUGAAU-3') for which the solution NMR structures are available (PDB:4BS2)⁴⁴. We
4
5 performed 15 independent simulations for each protein state (holo- or apo-) and pulling scenarios
6
7 (N-terminal or C-terminal pulling). Comparing the mean unfolding time of the apo-form when
8
9 stretched at a constant-force of $F = 160$ pN (grey trajectories) with that measured for the RNA-
10
11 bound protein (orange trajectories) displays a significant separation of timescales (Figure 4a,b),
12
13 suggesting that RNA binding slows down the mechanical unfolding of RRM1. In both cases,
14
15 pulling from the N-terminus leads to unfolding times that are noticeably larger than those
16
17 observed when the protein is pulled from the C-terminus (Figure 4a,b), implying that pulling
18
19 from both termini is not a fully-equivalent process, in the sense that the protein-nucleic acid
20
21 tandem (Figure 4c) resists better mechanical stress when the force propagates along the N- to the
22
23 C-termini direction (Figure 4d). Close investigation to the dynamics of the unfolding trajectories
24
25 put forward a rather unique mechanism of nucleic acid-mediated mechanical stabilization of
26
27 RRM1; in the apo- form, mechanical unfolding occurs upon disruption of the hydrogen bonds
28
29 present between $\beta 1$ and $\beta 5$. The protein geometry is such that the $\beta 1$ - $\beta 5$ strands are not aligned
30
31 with the direction of force application, resulting in a low cooperativity of the hydrogen-bonds
32
33 and thus very low mechanical resistance (unfolding occurs within ~ 10 ns in our simulations at F
34
35 = 160 pN, a force at which well-studied mechanically-resistant proteins such as the I27 markers
36
37 would not unfold in the simulations). In the native structure of the holo-RRM1, RNA binds
38
39 directly on top of $\beta 1$ and $\beta 5$, the protein region from where unfolding starts (Figure 4c,e).
40
41 Detailed scrutiny of the individual trajectories (Supplementary video1) shows that RNA acts as a
42
43 “molecular staple” that sits on top of the stretched RRM1, preventing its unfolding (Figure 4e,
44
45 *left*). Thermal fluctuations coupled with the mechanical stress applied to the protein eventually
46
47 displace RNA from this ‘lid’ well defined-position (Figure 4e, *middle*). Only after RNA has
48
49
50
51
52
53
54
55
56
57
58
59
60

1
2
3 been removed can the protein proceed to rapidly unfold and extend (Figure 4e, *right*). Hence,
4
5 RNA functions as an effective molecular ‘stopper’ that delays protein unfolding, occurring only
6
7 after RNA has been displaced from its binding position. As a further confirmation of this
8
9 mechanism, we performed 5 additional simulations where RNA was maintained fixed (Fig. S7).
10
11 No unfolding was observed in that case, whereas close to 100% of the traces in the presence of
12
13 flexible RNA unfolded on that same timescale.
14
15
16
17
18



1
2
3 **Figure 4.** (a) End-to-end as a function of time for 15 simulations in the apo state (grey) and 15
4 simulations in the holo state (orange), under a constant force of 160 pN, and pulling on the C-
5 terminal. Note that for trajectories where the protein did not unfold within the 40-ns time
6 window shown here, the simulations were extended until unfolding occurred. One trajectory of
7 the protein in the holo state is highlighted in red. (b) Same data but pulling on the N-terminal
8 instead, which shows a slight increase in mechanical resistance for both apo- and holo- cases. (c)
9 Solution NMR structure (PDB ID: 4BS2) of the RRM1 domain (grey) in complex with RNA
10 (orange), where the residues interacting with RRM2 in the structure have been removed. The N-
11 and C-terminal C_{α} , where force is applied (black arrows), are shown as blue balls. RRM1
12 mechanical unfolding is triggered by the loss of the interaction between $\beta 1$ and $\beta 5$. (d) Mean
13 unfolding times, showing that the presence of RNA considerably increases the mechanical
14 resistance of the RRM1 protein. Proteins are considered unfolded when their end-to-end distance
15 exceeds 3.5 nm (dashed black line in panels (a) and (b)). (e) Snapshots of protein/RNA
16 configurations at representative time intervals corresponding to an individual unfolding
17 trajectory (red in (a)): (*left*) stable initial intermediate before unfolding, showing that RNA acts as
18 a mechanical “lid” that momentarily blocks unfolding; local fluctuations of the RNA-protein
19 binding site allow detachment of $\beta 5$ from $\beta 1$ (*middle*), which triggers the subsequent unfolding
20 of the protein (*right*).

21
22
23
24
25
26
27
28
29
30
31
32
33
34
35
36
37
38
39
40
41
42
43
44
45
46
47 About 2% of the human proteome consists of DNA- and RNA- binding proteins
48 (DRBPs)³³. As expected, DRBPs are functionally flexible, and are mainly involved in
49 transcriptional regulation, mRNA processing and DNA replication. The versatile RRM (RNA
50 recognition motif) domain is the most enriched domain in DRBPs, underpinning a structure able
51
52
53
54
55
56
57
58
59
60

1
2
3 to simultaneously bind single stranded ssRNA and ssDNA, as well as proteins. TDP-43 is a
4 paradigmatic DRBP that has important roles in mRNA splicing⁴⁸ and miRNA biogenesis⁵², and
5 is formed by two independent RRM domains. Here we made use of multidisciplinary approach
6 including biochemistry and molecular biology techniques combined with single molecule
7 nanomechanical experiments complemented by SMD simulations to demonstrate that nucleic
8 acid binding can result in the mechanical stabilization of the RRM1 domain of TDP-43.
9
10
11
12
13
14
15
16
17
18

19 The main discovery of our single molecule experiments is that, under the presence of a
20 stretching force, the apo-form extends in a feature-less manner, demonstrating that the forces
21 required to unfold are lower than ~ 15 pN, the intrinsic resolution of the AFM working under
22 constant velocity conditions. Further work using e.g. optical or magnetic tweezers, with
23 expanded low-force resolution⁵³, could provide further insight into the individual unfolding
24 pathways of the apo-form of RRM1. By contrast, the addition of TG nucleotides results in a
25 remarkable mechanical stabilization of RRM1, giving rise to the characteristic saw-tooth pattern
26 of unfolding. However, the distribution of unfolding trajectories corresponding to the apo-form
27 (and also to the control experiments in the presence of CA) shows that a finite number of
28 unfolding events (~ 30 %) exhibiting mechanical resistance is always present. It is possible that
29 after our purification, and despite quantitative DNA removal⁴⁶, there is still a low fraction of
30 DNA-bound proteins. Conversely, in the presence of TG₁₅, we also observed a number of
31 unfolding events (~ 17 %) devoid of mechanical stability. We attribute these trajectories to the
32 presence of a dynamic binding/unbinding kinetics of the ssDNA oligonucleotides. Furthermore,
33 our titration experiments (Figure S3) demonstrate that, as expected, the short TG₃ shows a lower
34 binding affinity to RRM1 than TG₄, and that, in general, the binding affinity increases with the
35
36
37
38
39
40
41
42
43
44
45
46
47
48
49
50
51
52
53
54
55
56
57
58
59
60

1
2
3 length of the TG oligonucleotide. Notably, the different extent of binding of the TG
4 oligonucleotides of different lengths nicely correlates with the fraction of trajectories showing
5 mechanical stabilization (Figure 2c). Hence, an important conclusion stemming from our
6 experiments is that mechanical stability appears to be a direct reporter of DNA binding.
7
8
9
10
11
12
13
14

15 To obtain insight into the molecular origin of the mechanical stabilization process, we
16 conducted SMD simulations under force clamp conditions. Our simulations revealed a plausible
17 mechanism whereby the oligonucleotide binds directly onto the mechanical clamp of RRM1 (β 1
18 and β 5) and acts as a ‘mechanical lid’ that locks the protein, preventing unfolding. This
19 protective mechanism largely differs for example from the ‘allosteric’ binding mechanism
20 described for protein G, whereby the IgG ligand was found to bind on a position away from the
21 mechanical clamp²⁶. Thermal fluctuations coupled with the effects of the pulling force are able to
22 perturb the location of the nucleic acid, eventually slightly displacing it from the protein binding
23 site and thus allowing the detachment of β 5 from β 1, which triggers the subsequent unfolding of
24 the protein. Hence, given that mechanical stabilisation is mostly dictated by the residence time of
25 the oligonucleotide bound to RRM1, it is tempting to speculate that in the presence of
26 oligonucleotides able to bind RRM1 with high affinity (i.e. long TG repeats), the protein would
27 take longer to unfold, thus giving rise to an apparent higher mechanical stability under force
28 extension conditions. Indeed, close inspection to the histograms reporting the experimental
29 unfolding forces for the different TG constructs (Figure S4 and Table S1) shows an overall
30 significant ($p < 0.05$) increase of mechanical stability for those constructs with longer TG
31 repeats, shifting from ~ 25 pN for TG₃ up to ~ 40 pN in the case of TG₁₅, thus qualitatively
32 supporting the bound-stabilization argument. From the experimental perspective, it remains to be
33
34
35
36
37
38
39
40
41
42
43
44
45
46
47
48
49
50
51
52
53
54
55
56
57
58
59
60

1
2
3 seen whether RNA binding gives rise to a similar mechanical stabilization to that obtained by
4 DNA-related sequences. A further interesting feature observed in our long simulations is that,
5
6 DNA-related sequences. A further interesting feature observed in our long simulations is that,
7
8 after being displaced from the binding pocket enabling protein unfolding, the oligonucleotide is
9
10 kept bound to the mechanically stretched protein (Supplementary video 1). It is hence possible
11
12 that the relatively fast rebinding that we observed in our force-clamp experiments (Figure 3a)
13
14 occurs because the oligonucleotide remains bound after mechanical unfolding, hence rendering
15
16 the rebinding process more efficient.
17
18
19
20
21

22 From a broader perspective, our findings demonstrate that, akin to the mechanical stabilization
23
24 effect triggered by protein-binding¹², nucleic acid binding can also have a drastic effect on the
25
26 mechanical stability of proteins. Most significantly, our results show that, rather than changing
27
28 the unfolding pathway as observed in the case of p53³⁴, DNA binding can directly affect the
29
30 mechanical stability of a protein under force. Given the emerging role of the nucleus as a
31
32 mechanosensor⁵⁴⁻⁵⁵, and in light of recent discoveries evidencing that external mechanical
33
34 perturbations can trigger gene expression after DNA remodelling⁵⁶⁻⁵⁸, it is at least tantalising to
35
36 hypothesize that nucleic acid binding can have important effects on the conformational dynamics
37
38 of e.g transcription factors. In particular, it is plausible that such a conformational stabilization
39
40 can play a key role in the dynamics of exon 9 skipping of the human *CFTR* gene, in the
41
42 regulation of which TDP-43 plays a key role^{48, 50}. Although almost all the ALS and FTD
43
44 pathological mutations map to the intrinsically disordered C-terminal region and also to the
45
46 RRM2⁵⁹ and N-terminal domain of TDP-43⁶⁰, the delayed unfolding upon DNA binding
47
48 demonstrated here for RRM1 might be generally related to a delayed onset or inhibition of TDP-
49
50 43 aggregation⁴⁹ –the hallmark of amyotrophic lateral sclerosis (ALS) and frontotemporal lobar
51
52
53
54
55
56
57
58
59
60

1
2
3 degeneration (FTLD). Moreover, it is also possible that the TDP-43 stabilization upon nucleic
4 acid binding that we observe might be related to the increased solubilization of nuclear TDP-
5
6
7 43⁶¹. Further single molecule experiments on the other regions of the TDP-43 protein, directed to
8
9
10 elucidate how nucleic acid binding affects the nanomechanical properties of the RRM2, the C-
11
12 terminal region and the NLS sequence⁴², would increase the biological relevance of the reported
13
14 findings. From a strict mechanical viewpoint, our results suggest a new rational way to modulate
15
16 the mechanical properties of proteins to add to post-translational modifications⁶²⁻⁶⁴ or ligand
17
18 binding¹², and highlights the use of protein mechanical stability as an emerging molecular
19
20 reporter of nucleic acid binding to proteins.
21
22
23
24
25

26 ASSOCIATED CONTENT

31 **Supporting Information.**

32
33 Supplementary material for this article is available at:

34
35 Materials and Methods

36
37 Figure S1. Distribution of the increment in contour length values associated to the unfolding of
38 RRM.

39
40 Figure S2. Gallery of unfolding trajectories of the [I27₂-RRM1-I27-RRM1-I27₂] polyprotein.

41
42 Figure S3. Protein:DNA titrations monitored by EMSA.

43
44 Figure S4. Distribution of unfolding forces for those trajectories featuring mechanical stability.

45
46 Figure S5. Distributions of the step size (a) and force (b) associated to the unfolding of RRM1 in
47 the TG₁₅-bound holo- form in the force ramp experiment.

48
49 Figure S6. Refolding trajectory of the [I27₂-RRM1-I27-RRM1-I27₂] polyprotein in the presence
50 of TG₆.

51
52 Figure S7. Simulation of the end-to-end distance as a function of time for proteins with frozen
53 RNA.

54
55 Table S1. Statistical analysis of the unfolding forces under the different experimental conditions.
56
57
58
59
60

1
2
3 Supplementary Movie 1. Individual SMD trajectory of RRM1 unfolding in the presence of RNA.
4
5
6
7

8 AUTHOR INFORMATION
9

10 The authors declare no competing commercial interests.
11
12

13 ACKNOWLEDGMENTS
14
15

16 We thank Dr. Amy Beedle for help in discussion of the results and critical reading of the
17 manuscript. G.S. acknowledges support from CNRS through a PICS allocation (PICS07571) and
18 from the "Initiative d'Excellence" program from the French State (Grant "DYNAMO", ANR-11-
19 LABX-0011-01). This work was supported by the BBSRC grant BB/J00992X/1, BHF grant
20 (PG/13/50/30426), EPSRC Fellowship K00641X/1, by the European Commission (grant
21 agreement SEP-210342844), and by the Leverhulme Trust Research Leadership Award (RL-
22 2016-015), all to S.G-M.
23
24
25
26
27
28
29
30
31

32 REFERENCES
33
34

- 35
36 1. Vogel, V., Mechanotransduction involving multimodular proteins: converting force into
37 biochemical signals. *Annu Rev Biophys Biomol Struct* **2006**, *35*, 459-88.
38 2. Roca-Cusachs, P.; Iskratsch, T.; Sheetz, M. P., Finding the weakest link: exploring
39 integrin-mediated mechanical molecular pathways. *J Cell Sci* **2012**, *125*, 3025-38.
40 3. Li, H.; Linke, W. A.; Oberhauser, A. F.; Carrion-Vazquez, M.; Kerkvliet, J. G.; Lu, H.;
41 Marszalek, P. E.; Fernandez, J. M., Reverse engineering of the giant muscle protein titin. *Nature*
42 **2002**, *418*, 998-1002.
43 4. Aubin-Tam, M. E.; Olivares, A. O.; Sauer, R. T.; Baker, T. A.; Lang, M. J., Single-
44 molecule protein unfolding and translocation by an ATP-fueled proteolytic machine. *Cell* **2011**,
45 *145*, 257-67.
46 5. Maillard, R. A.; Chistol, G.; Sen, M.; Righini, M.; Tan, J.; Kaiser, C. M.; Hodges, C.;
47 Martin, A.; Bustamante, C., ClpX(P) generates mechanical force to unfold and translocate its
48 protein substrates. *Cell* **2011**, *145*, 459-69.
49 6. Stirnemann, G.; Giganti, D.; Fernandez, J. M.; Berne, B. J., Elasticity, structure, and
50 relaxation of extended proteins under force. *Proc Natl Acad Sci U S A* **2013**, *110*, 3847-52.
51 7. Li, H.; Carrion-Vazquez, M.; Oberhauser, A. F.; Marszalek, P. E.; Fernandez, J. M.,
52 Point mutations alter the mechanical stability of immunoglobulin modules. *Nat Struct Biol* **2000**,
53 *7*, 1117-20.
54
55
56
57
58
59
60

- 1
- 2
- 3
- 4 8. Carl, P.; Kwok, C. H.; Manderson, G.; Speicher, D. W.; Discher, D. E., Forced unfolding
- 5 modulated by disulfide bonds in the Ig domains of a cell adhesion molecule. *Proc Natl Acad Sci*
- 6 *U S A* **2001**, *98*, 1565-70.
- 7
- 8 9. Wiita, A. P.; Ainavarapu, S. R.; Huang, H. H.; Fernandez, J. M., Force-dependent
- 9 chemical kinetics of disulfide bond reduction observed with single-molecule techniques. *Proc*
- 10 *Natl Acad Sci U S A* **2006**, *103*, 7222-7.
- 11
- 12 10. Zheng, P.; Li, H., Highly covalent ferric-thiolate bonds exhibit surprisingly low
- 13 mechanical stability. *J Am Chem Soc* **2011**, *133*, 6791-8.
- 14
- 15 11. Beedle, A. E.; Lezamiz, A.; Stirnemann, G.; Garcia-Manyes, S., The mechanochemistry
- 16 of copper reports on the directionality of unfolding in model cupredoxin proteins. *Nat Commun*
- 17 **2015**, *6*, 7894.
- 18
- 19 12. Hu, X.; Li, H., Force spectroscopy studies on protein-ligand interactions: a single protein
- 20 mechanics perspective. *FEBS Lett* **2014**, *588*, 3613-20.
- 21
- 22 13. Ainavarapu, S. R.; Li, L.; Badilla, C. L.; Fernandez, J. M., Ligand binding modulates the
- 23 mechanical stability of dihydrofolate reductase. *Biophys J* **2005**, *89*, 3337-44.
- 24
- 25 14. Wang, C. C.; Tsong, T. Y.; Hsu, Y. H.; Marszalek, P. E., Inhibitor binding increases the
- 26 mechanical stability of staphylococcal nuclease. *Biophys J* **2011**, *100*, 1094-9.
- 27
- 28 15. Bertz, M.; Rief, M., Ligand binding mechanics of maltose binding protein. *J Mol Biol*
- 29 **2009**, *393*, 1097-105.
- 30
- 31 16. Aggarwal, V.; Kulothungan, S. R.; Balamurali, M. M.; Saranya, S. R.; Varadarajan, R.;
- 32 Ainavarapu, S. R., Ligand-modulated parallel mechanical unfolding pathways of maltose-
- 33 binding proteins. *J Biol Chem* **2011**, *286*, 28056-65.
- 34
- 35 17. Rivas-Pardo, J. A.; Alegre-Cebollada, J.; Ramirez-Sarmiento, C. A.; Fernandez, J. M.;
- 36 Guixé, V., Identifying sequential substrate binding at the single-molecule level by enzyme
- 37 mechanical stabilization. *ACS Nano* **2015**, *9*, 3996-4005.
- 38
- 39 18. Zoicher, M.; Zhang, C.; Rasmussen, S. G.; Kobilka, B. K.; Muller, D. J., Cholesterol
- 40 increases kinetic, energetic, and mechanical stability of the human beta2-adrenergic receptor.
- 41 *Proc Natl Acad Sci U S A* **2012**, *109*, E3463-72.
- 42
- 43 19. Kotamarthi, H. C.; Sharma, R.; Narayan, S.; Ray, S.; Ainavarapu, S. R., Multiple
- 44 unfolding pathways of leucine binding protein (LBP) probed by single-molecule force
- 45 spectroscopy (SMFS). *J Am Chem Soc* **2013**, *135*, 14768-74.
- 46
- 47 20. Junker, J. P.; Rief, M., Single-molecule force spectroscopy distinguishes target binding
- 48 modes of calmodulin. *Proc Natl Acad Sci U S A* **2009**, *106*, 14361-6.
- 49
- 50 21. Junker, J. P.; Ziegler, F.; Rief, M., Ligand-dependent equilibrium fluctuations of single
- 51 calmodulin molecules. *Science* **2009**, *323*, 633-7.
- 52
- 53 22. Ramanujam, V.; Kotamarthi, H. C.; Ainavarapu, S. R., Ca²⁺ binding enhanced
- 54 mechanical stability of an archaeal crystallin. *PLoS One* **2014**, *9*, e94513.
- 55
- 56 23. Oroz, J.; Valbuena, A.; Vera, A. M.; Mendieta, J.; Gomez-Puertas, P.; Carrion-Vazquez,
- 57 M., Nanomechanics of the cadherin ectodomain: "canalization" by Ca²⁺ binding results in a new
- 58 mechanical element. *J Biol Chem* **2011**, *286*, 9405-18.
- 59
- 60 24. Cao, Y.; Yoo, T.; Li, H., Single molecule force spectroscopy reveals engineered metal
- chelation is a general approach to enhance mechanical stability of proteins. *Proc Natl Acad Sci U*
- S A* **2008**, *105*, 11152-7.
25. Cao, Y.; Li, Y. D.; Li, H., Enhancing the mechanical stability of proteins through a
- cocktail approach. *Biophys J* **2011**, *100*, 1794-9.

- 1
2
3 26. Cao, Y.; Li, H., Engineered elastomeric proteins with dual elasticity can be controlled by
4 a molecular regulator. *Nat Nanotechnol* **2008**, *3*, 512-6.
5 27. Kotamarthi, H. C.; Yadav, A.; Koti Ainarapu, S. R., Small peptide binding stiffens the
6 ubiquitin-like protein SUMO1. *Biophys J* **2015**, *108*, 360-7.
7 28. Perales-Calvo, J.; Lezamiz, A.; Garcia-Manyes, S., The Mechanochemistry of a
8 Structural Zinc Finger. *J Phys Chem Lett* **2015**, *6*, 3335-40.
9 29. Friedland, J. C.; Lee, M. H.; Boettiger, D., Mechanically activated integrin switch
10 controls alpha5beta1 function. *Science* **2009**, *323*, 642-4.
11 30. del Rio, A.; Perez-Jimenez, R.; Liu, R.; Roca-Cusachs, P.; Fernandez, J. M.; Sheetz, M.
12 P., Stretching single talin rod molecules activates vinculin binding. *Science* **2009**, *323*, 638-41.
13 31. Yao, M.; Qiu, W.; Liu, R.; Efremov, A. K.; Cong, P.; Seddiki, R.; Payre, M.; Lim, C. T.;
14 Ladoux, B.; Mege, R. M.; Yan, J., Force-dependent conformational switch of alpha-catenin
15 controls vinculin binding. *Nat Commun* **2014**, *5*, 4525.
16 32. Bechtluft, P.; van Leeuwen, R. G.; Tyreman, M.; Tomkiewicz, D.; Nouwen, N.; Tepper,
17 H. L.; Driessen, A. J.; Tans, S. J., Direct observation of chaperone-induced changes in a protein
18 folding pathway. *Science* **2007**, *318*, 1458-61.
19 33. Hudson, W. H.; Ortlund, E. A., The structure, function and evolution of proteins that bind
20 DNA and RNA. *Nat Rev Mol Cell Biol* **2014**, *15*, 749-60.
21 34. Taniguchi, Y.; Kawakami, M., Variation in the mechanical unfolding pathway of
22 p53DBD induced by interaction with p53 N-terminal region or DNA. *PLoS One* **2012**, *7*,
23 e49003.
24 35. Wang, I. F.; Wu, L. S.; Shen, C. K., TDP-43: an emerging new player in
25 neurodegenerative diseases. *Trends Mol Med* **2008**, *14*, 479-85.
26 36. Buratti, E.; Baralle, F. E., TDP-43: gumming up neurons through protein-protein and
27 protein-RNA interactions. *Trends Biochem Sci* **2012**, *37*, 237-47.
28 37. Warraich, S. T.; Yang, S.; Nicholson, G. A.; Blair, I. P., TDP-43: a DNA and RNA
29 binding protein with roles in neurodegenerative diseases. *Int J Biochem Cell Biol* **2010**, *42*,
30 1606-9.
31 38. Neumann, M.; Sampathu, D. M.; Kwong, L. K.; Truax, A. C.; Micsenyi, M. C.; Chou, T.
32 T.; Bruce, J.; Schuck, T.; Grossman, M.; Clark, C. M.; McCluskey, L. F.; Miller, B. L.; Masliah,
33 E.; Mackenzie, I. R.; Feldman, H.; Feiden, W.; Kretzschmar, H. A.; Trojanowski, J. Q.; Lee, V.
34 M., Ubiquitinated TDP-43 in frontotemporal lobar degeneration and amyotrophic lateral
35 sclerosis. *Science* **2006**, *314*, 130-3.
36 39. Banks, G. T.; Kuta, A.; Isaacs, A. M.; Fisher, E. M., TDP-43 is a culprit in human
37 neurodegeneration, and not just an innocent bystander. *Mamm Genome* **2008**, *19* (5), 299-305.
38 40. Ederle, H.; Dormann, D., TDP-43 and FUS en route from the nucleus to the cytoplasm.
39 *FEBS Lett* **2017**, *591*, 1489-1507.
40 41. Passoni, M.; De Conti, L.; Baralle, M.; Buratti, E., UG repeats/TDP-43 interactions near
41 5' splice sites exert unpredictable effects on splicing modulation. *J Mol Biol* **2012**, *415*, 46-60.
42 42. Mompean, M.; Romano, V.; Pantoja-Uceda, D.; Stuani, C.; Baralle, F. E.; Buratti, E.;
43 Laurents, D. V., The TDP-43 N-terminal domain structure at high resolution. *FEBS J* **2016**, *283*,
44 1242-60.
45 43. Kuo, P. H.; Doudeva, L. G.; Wang, Y. T.; Shen, C. K.; Yuan, H. S., Structural insights
46 into TDP-43 in nucleic-acid binding and domain interactions. *Nucleic Acids Res* **2009**, *37*, 1799-
47 808.
48
49
50
51
52
53
54
55
56
57
58
59
60

- 1
2
3 44. Lukavsky, P. J.; Daujotyte, D.; Tollervey, J. R.; Ule, J.; Stuani, C.; Buratti, E.; Baralle, F.
4 E.; Damberger, F. F.; Allain, F. H., Molecular basis of UG-rich RNA recognition by the human
5 splicing factor TDP-43. *Nat Struct Mol Biol* **2013**, *20*, 1443-9.
- 6 45. Kuo, P. H.; Chiang, C. H.; Wang, Y. T.; Doudeva, L. G.; Yuan, H. S., The crystal
7 structure of TDP-43 RRM1-DNA complex reveals the specific recognition for UG- and TG-rich
8 nucleic acids. *Nucleic Acids Res* **2014**, *42*, 4712-22.
- 9 46. Glasel, J. A., Validity of nucleic acid purities monitored by 260nm/280nm absorbance
10 ratios. *Biotechniques* **1995**, *18*, 62-3.
- 11 47. Carrion-Vazquez, M.; Oberhauser, A. F.; Fowler, S. B.; Marszalek, P. E.; Broedel, S. E.;
12 Clarke, J.; Fernandez, J. M., Mechanical and chemical unfolding of a single protein: a
13 comparison. *Proc Natl Acad Sci U S A* **1999**, *96*, 3694-9.
- 14 48. Buratti, E.; Dork, T.; Zuccato, E.; Pagani, F.; Romano, M.; Baralle, F. E., Nuclear factor
15 TDP-43 and SR proteins promote in vitro and in vivo CFTR exon 9 skipping. *EMBO J* **2001**, *20*,
16 1774-84.
- 17 49. Huang, Y. C.; Lin, K. F.; He, R. Y.; Tu, P. H.; Koubek, J.; Hsu, Y. C.; Huang, J. J.,
18 Inhibition of TDP-43 aggregation by nucleic acid binding. *PLoS One* **2013**, *8*, e64002.
- 19 50. Buratti, E.; Baralle, F. E., Characterization and functional implications of the RNA
20 binding properties of nuclear factor TDP-43, a novel splicing regulator of CFTR exon 9. *J Biol*
21 *Chem* **2001**, *276*, 36337-43.
- 22 51. Fernandez, J. M.; Li, H., Force-clamp spectroscopy monitors the folding trajectory of a
23 single protein. *Science* **2004**, *303*, 1674-8.
- 24 52. Kawahara, Y.; Mieda-Sato, A., TDP-43 promotes microRNA biogenesis as a component
25 of the Drosha and Dicer complexes. *Proc Natl Acad Sci U S A* **2012**, *109*, 3347-52.
- 26 53. Rivas-Pardo, J. A.; Eckels, E. C.; Popa, I.; Kosuri, P.; Linke, W. A.; Fernandez, J. M.,
27 Work Done by Titin Protein Folding Assists Muscle Contraction. *Cell Rep* **2016**, *14*, 1339-1347.
- 28 54. Fedorchak, G. R.; Kaminski, A.; Lammerding, J., Cellular mechanosensing: getting to the
29 nucleus of it all. *Prog Biophys Mol Biol* **2014**, *115*, 76-92.
- 30 55. Cho, S.; Irianto, J.; Discher, D. E., Mechanosensing by the nucleus: From pathways to
31 scaling relationships. *J Cell Biol* **2017**, *216*, 305-315.
- 32 56. Tajik, A.; Zhang, Y.; Wei, F.; Sun, J.; Jia, Q.; Zhou, W.; Singh, R.; Khanna, N.; Belmont,
33 A. S.; Wang, N., Transcription upregulation via force-induced direct stretching of chromatin. *Nat*
34 *Mater* **2016**, *15*, 1287-1296.
- 35 57. Poh, Y. C.; Shevtsov, S. P.; Chowdhury, F.; Wu, D. C.; Na, S.; Dunder, M.; Wang, N.,
36 Dynamic force-induced direct dissociation of protein complexes in a nuclear body in living cells.
37 *Nat Commun* **2012**, *3*, 866.
- 38 58. Jain, N.; Iyer, K. V.; Kumar, A.; Shivashankar, G. V., Cell geometric constraints induce
39 modular gene-expression patterns via redistribution of HDAC3 regulated by actomyosin
40 contractility. *Proc Natl Acad Sci U S A* **2013**, *110*, 11349-54.
- 41 59. Guenther, E. L.; Ge, P.; Trinh, H.; Sawaya, M. R.; Cascio, D.; Boyer, D. R.; Gonen, T.;
42 Zhou, Z. H.; Eisenberg, D. S., Atomic-level evidence for packing and positional amyloid
43 polymorphism by segment from TDP-43 RRM2. *Nat Struct Mol Biol* **2018**, *25*, 311-319.
- 44 60. Wang, A.; Conicella, A. E.; Schmidt, H. B.; Martin, E. W.; Rhoads, S. N.; Reeb, A. N.;
45 Nourse, A.; Ramirez Montero, D.; Ryan, V. H.; Rohatgi, R.; Shewmaker, F.; Naik, M. T.;
46 Mittag, T.; Ayala, Y. M.; Fawzi, N. L., A single N-terminal phosphomimic disrupts TDP-43
47 polymerization, phase separation, and RNA splicing. *EMBO J* **2018**, *37*, e97452.
- 48
49
50
51
52
53
54
55
56
57
58
59
60

- 1
2
3 61. Maharana, S.; Wang, J.; Papadopoulos, D. K.; Richter, D.; Pozniakovsky, A.; Poser, I.;
4 Bickle, M.; Rizk, S.; Guillen-Boixet, J.; Franzmann, T. M.; Jahnel, M.; Marrone, L.; Chang, Y.
5 T.; Sternecker, J.; Tomancak, P.; Hyman, A. A.; Alberti, S., RNA buffers the phase separation
6 behavior of prion-like RNA binding proteins. *Science* **2018**, *360*, 918-921.
7
8 62. Alegre-Cebollada, J.; Kosuri, P.; Giganti, D.; Eckels, E.; Rivas-Pardo, J. A.; Hamdani,
9 N.; Warren, C. M.; Solaro, R. J.; Linke, W. A.; Fernandez, J. M., S-glutathionylation of cryptic
10 cysteines enhances titin elasticity by blocking protein folding. *Cell* **2014**, *156*, 1235-1246.
11 63. Beedle, A. E.; Lynham, S.; Garcia-Manyes, S., Protein S-sulfenylation is a fleeting
12 molecular switch that regulates non-enzymatic oxidative folding. *Nat Commun* **2016**, *7*, 12490.
13 64. Beedle, A. E. M.; Mora, M.; Lynham, S.; Stirnemann, G.; Garcia-Manyes, S., Tailoring
14 protein nanomechanics with chemical reactivity. *Nat Commun* **2017**, *8*, 15658.
15
16
17
18
19
20
21
22
23
24
25
26
27
28
29
30
31
32
33
34
35
36
37
38
39
40
41
42
43
44
45
46
47
48
49
50
51
52
53
54
55
56
57
58
59
60